Original Article

Institution of MECHANICAL ENGINEERS
Journal of AUTOMOBILE ENGINEERING

Proc IMechE Part D:
J Automobile Engineering
2014, Vol. 228(11) 1274–1284
© IMechE 2014
Reprints and permissions:
sagepub.co.uk/journalsPermissions.nav
DOI: 10.1177/0954407014530894
pid.sagepub.com
SAGE

Experimental investigations on the increase in nitric oxide emissions using biodiesels and their mitigation

Thangaraja Jeyaseelan, Anand Krishnasamy and Pramod S Mehta

Abstract

One of the major shortcomings to be addressed in the widespread applications of biodiesel fuel for compression ignition engines is the formation of higher nitric oxide emissions. It is well established in the literature that thermal nitric oxide is a dominant source for nitric oxide formation in engines. Thermal nitric oxide formation increases by any in-cylinder combustion strategy that alters the in-cylinder temperatures, the oxygen fraction or the residence time of high-temperature post-flame burned gases. The differences between the properties of biodiesel in terms of a higher bulk modulus, a higher cetane number and the presence of a fuel-bound oxygen fraction and the properties of diesel are found to affect the in-cylinder charge conditions and thus the nitric oxide formation. The present work aims to understand the major contributor to the higher nitric oxide formation with biodiesel based on experimental investigations in two different engine configurations: one with a conventional mechanical-type injection system and the other with a modern common-rail direct-injection system. The experimental results highlight that the dynamic injection timing advanced up to a maximum of 2.6° crank angle owing to the higher bulk modulus of biodiesel. This factor contributes to specific nitric oxide emissions which are 7.5% higher in an engine having a mechanical-type injection system. The increase in the nitric oxide is neutralized on restoring the injection timing to that of the diesel injection time setting. In the case of an engine with a modern common-rail direct-injection system, the injection timings remain unaltered, and the nitric oxide concentrations for diesel and for biodiesel–diesel blends also remains the same.

Keywords

Karanja biodiesel, injection timings, common-rail direct-injection system, thermal nitric oxide, peak pressure

Date received: 25 October 2013; accepted: 17 March 2014

Introduction

Owing to the renewable nature,[1] biodiesel fuels derived from vegetable oils or animal fats have attracted significant attention as alternatives to fossil diesel fuel for use in compression ignition engines. Biodiesel fuels contain mono-alkyl esters of long-chain fatty acids and meet the requirements for engine fuels in accordance with the standards ASTM D6751[2] and EN 14214:2008.[3] Use of biodiesel in a compression ignition engine reduces the carbon monoxide, unburned hydrocarbon and particulate matter emissions[4] but contributes to higher nitric oxide (NO) emissions. The US Environmental Protection Agency report[5] on heavy-duty diesel engines points out that with the use of neat biodiesel there is generally a 10% increase in the nitrogen oxide (NO_x) emissions compared with the use of diesel. The major attributes for higher NO_x emissions in biodiesel-fuelled engines are the variations in the fuel properties in terms of a higher density, a lower energy content, a lower volatility, a higher iodine number[6,7] and a faster burn rate because of the presence of fuel-bound oxygen.[8,9] Knight et al.[10] investigated the NO_x emissions using palm olein biodiesel in a medium-duty common-rail direct-injection (CRDI) engine fitted with a variable-geometry rotor and an exhaust gas recirculation (EGR) cooler. They classified the effect of the biodiesel NO_x penalty with respect to the fundamental factors versus the fuel properties (namely the ignition delay and the

Department of Mechanical Engineering, Indian Institute of Technology Madras, Chennai, India

Corresponding author:
Pramod S Mehta, Internal Combustion Engine Laboratory, Department of Mechanical Engineering, Indian Institute of Technology Madras, Chennai 600036, India.
Email: psmehta@iitm.ac.in

Downloaded from pid.sagepub.com at University of Sydney on May 1, 2015

Table 1. Injection advance with biodiesel relative to diesel fuel.

Investigator(s)	Biodiesel	Injection advance (deg CA)	Changes attributed to the following
Monyem et al.[11]	Soybean oil	2.30	Lower compressibility
Canakci and Van Gerpen[12]	Soybean oil	2.68	Changes in the physical properties
	Yellow grease	3.55	
Szybist et al.[13]	Soybean oil	1–1.2	Difference in the bulk modulus
Anand et al.[14]	Karanja oil	2.30	Higher density, resulting in faster travel of the acoustic pressure waves
Dhar and Agarwal[15]	Karanja oil	1.76[a]	Higher bulk modulus, viscosity and sonic velocity

CA: crank angle.
[a]Obtained from a graph for idling at 2600 r/min.

combustion duration) and also to the engine parameters (namely the injection timing, the rail pressure and the EGR rate) in various operating conditions. They concluded that biodiesel fundamentally poses the tendency to emit higher NO_x emissions. Experimental investigations by several researchers using different types of biodiesel fuel in engines with similar injection time settings as that of diesel revealed that there is an automatic injection advance with biodiesel operation due to the differences in the fuel properties (primarily the bulk modulus) (Table 1).

Sun et al.[16] reviewed the formation of higher NO_x emissions with biodiesel fuels and concluded that the changes in the injection timing, the adiabatic flame temperature, the radiation heat transfer and the ignition delay are the various parameters influencing its formation. They also highlighted that the smaller differences between the fuel properties of biodiesel and diesel are sufficient to create several changes in the engine combustion characteristics. Further, they observed inconsistent trends in the reported literature with respect to the NO_x emissions with different biodiesel fuels.

Ren et al.[17] used 41 species and 150 reaction mechanisms for methyl butanoate as a biodiesel surrogate and *n*-heptane as a diesel surrogate to understand the effects of the physical and chemical properties of biodiesel fuels on the combustion and emissions formation processes. Their results showed that the differences in the physical properties of the biodiesel fuels influence their spray and atomization processes as well as the diffusive combustion phase relative to the corresponding characteristics of diesel fuel. Similarly, the variations in the chemical properties change the combustion parameters. More importantly, they opined that the differences between the chemical properties of biodiesel and those of diesel are responsible for a higher NO concentration. Canakci[18] concluded that one of the major reasons for the higher NO_x formation with biodiesel fuel is its fuel-bound oxygen content since it may provide additional oxygen for the formation of NO_x.

The earlier investigations and recent review articles[19,20] reporting higher NO emissions in biodiesel-fuelled engines highlighted several factors responsible for its formation. However, it becomes important to understand a major contributing factor or property to the higher NO emissions from biodiesel in order to mitigate it, using appropriate methodologies as outlined by Palash et al.[21]

This paper attempts to identify the major factor responsible for higher NO emissions with Karanja biodiesel based on the experimental investigations in two different engines: one with a conventional mechanical-type injection system and the other with a modern CRDI system.

Experimental set-up

The experiments are conducted on an Eicher diesel engine with a mechanical-type injection system and a Ford diesel engine having an electronic injection system, the specifications of which are provided in Table 2. The Eicher engine is a typical high-load low-speed truck diesel engine which meets Bharat stage II emission norms, and the Ford engine is a typical modern passenger car engine meeting Bharat stage IV emission standards.

Engine A is equipped with a mechanical-distributor-type fuel pump which distributes high-pressure fuel into the individual cylinders through fuel injectors having five symmetric holes along their periphery. Engine B consists of an electronically controlled piezo injector which is capable of injecting the fuel at a maximum injection pressure of 100 MPa with the help of a high-pressure pump. The injection system is capable of providing a double injection, namely a pilot injection and a main injection. The engine has an electronic control unit which controls the entire engine operation based on the engine mapping. A centrifugal pump is used to provide forced circulation cooling for the engine and the dynamometer. The cooling water is pumped from a water tank and circulated through the cooling passages provided in the engine and the dynamometer. A schematic arrangement of the engine test set-up is shown in Figure 1.

Both the engines are fitted with Dynalec eddy-current-type dynamometers together with electronic controllers for controlling the engine's operating speed and load. The engines are instrumented for both performance and in-cylinder pressure measurements. While a calibrated strain gauge load sensor is used for torque

Downloaded from pid.sagepub.com at University of Sydney on May 1, 2015

Table 2. Test engine specifications.

Specification	Description or value for the following engines	
	A (mechanical injection system)	B (electronic injection system)
Engine		
Make and model	Eicher E483 (truck applications)	Ford DV3 (passenger cars)
Engine type	Four-cylinder, in-line turbocharged, direct-injection compression ignition; four stroke and four valves per cylinder	Four-cylinder, in-line turbocharged, direct-injection compression ignition; four stroke and four valves per cylinder
Bore (mm)	100	73.7
Stroke (mm)	105	82
Displacement (cm^3)	3298	1399
Compression ratio	17.5:1	18.1:1
Maximum torque condition (N m)	285 at 1400 r/min	160 at 2000 r/min
Maximum power condition (kW)	70 at 200 r/min	50.72 at 4000 r/min
Injection system		
Fuel pump type	Distributor system	Common-rail system
Nozzle-opening pressure	230 bar	1000 bar (maximum injection pressure)
Number of injector holes	5	6
Injector diameter (mm)	0.209	0.122
Injection timing (static) (deg CA bTDC)	12	

CA: crank angle: bTDC: before top dead centre.

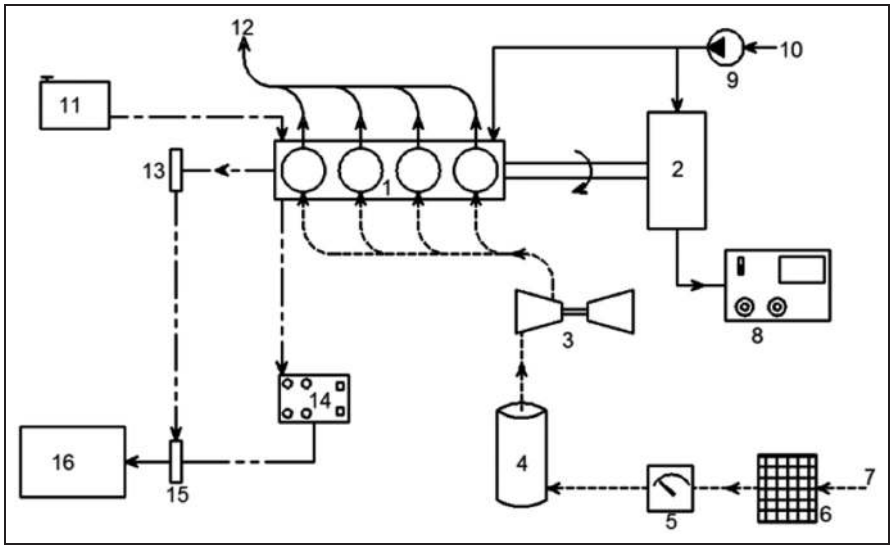

Figure 1. Schematic diagram of the engine experimental set-up: 1, four-cylinder engine; 2, eddy current dynamometer; 3, turbocharger; 4, surge tank; 5, turbine meter; 6, air filter; 7, air inlet; 8, dynamo controller; 9, water pump; 10, water inlet; 11, fuel tank; 12, exhaust outlet–turbine inlet; 13, crank angle encoder; 14, signal conditioner; 15, data acquisition unit; 16, personal computer.

measurement, a magnetic pick-up pulse sensor measures the engine speed. Kistler piezoelectric pressure transducers are used for measuring the in-cylinder pressure histories, while Kistler piezoresistive transducers are used for measuring the intake and fuel line pressures. The fuel flow rates and the air flow rates are measured using a burette–stopwatch arrangement and a turbine meter respectively.

The start-of-injection timing for engine B is obtained from a KiBox analyser which receives a signal from a current clamp adapter (E3N clamp), connected to an injector wiring harness. The other injection parameters concerning the injection schedule such as the duration of the pilot injection, the dwell between the pilot injection pulse and the main injection pulse and the duration of the main injection are recorded with an oscilloscope by measuring the voltage across the supply lines leading to the injectors from the electronic control unit.

The temperatures of the exhaust gas, the lubricant oil, the cooling water and the inlet air are measured using K-type thermocouples in order to monitor engine

Downloaded from pid.sagepub.com at University of Sydney on May 1, 2015

Table 3. Test matrix and fuel types.

Engine type	Operating conditions
A (mechanical injection system)	BMEP, 0.15 MPa, 0.31 MPa, 0.47 MPa, 0.63 MPa, 0.78 MPa at 2500 r/min
Fuel type	Diesel and K100
B (electronic injection system)	BMEP, 0.2 MPa, 0.4 MPa, 0.6 MPa, 0.8 MPa, 0.10 MPa at 2000 r/min
Fuel type	Diesel and K50D50

BMEP: brake mean effective pressure; K100: Karanja biodiesel; K50D50: 50 vol % Karanja biodiesel–50 vol % diesel.

operation. The analogue signals from the various pressure sensors are fed through a signal conditioner to a KiBox combustion analyser for online monitoring of engine operation as well as for post-processing the recorded data. For the test engine A an alternative inductive sensor and a 60-2 toothed wheel (designed in house) were used to provide the phasing signal required for acquiring the pressure data.

Experimental methodology

All the data are acquired at a fixed crank angle (CA) interval of 0.1°. The raw cylinder pressure and the fuel line pressure histories recorded in the KiBox analyser are averaged over 100 consecutive cycles with the help of a dedicated MATLAB program. The exhaust NO concentrations are measured using a chemilumniscent-type analyser (Rosemount 951A).

The apparent net heat release rates Q_{net} are estimated from the measured cylinder pressure histories by using the first law of thermodynamics applicable to the closed part of engine cycle expressed as

$$\frac{\mathrm{d}Q_{net}}{\mathrm{d}t} = \frac{n}{n-1}p\frac{\mathrm{d}V}{\mathrm{d}t} + \frac{1}{n-1}V\frac{\mathrm{d}p}{\mathrm{d}t} \quad (1)$$

where n is the polytrophic index, p is the instantaneous cylinder pressure and V is the instantaneous cylinder volume. The injection and cylinder pressure histories in conjunction with the energy release diagrams form the basis of the desired combustion parameters, namely the peak cylinder pressure and its occurrence, the start of injection, the ignition delay and the combustion phasing. In this investigation, the slope changeover point in the plot of the first derivative of the pressure is used to define the start of combustion. The variations in the dynamic start of injection are inferred from the fuel line pressures histories by considering the instant at which the line pressure attains the prescribed injector nozzle-opening pressure of 23 MPa. Based on similar investigations by earlier researchers, it was known that, owing to the effects of the changes in the fuel properties, the maximum injection advance with biodiesel fuels are found to be approximately 2° CA (see Table 1) which is taken as baseline data to retard the injection timing in the present work. The injection retard in the distributor-pump-type injection system is achieved manually by anticlockwise rotation (viewed from the flywheel end) of the whole pump assembly. The same injection timing as that of diesel timing was confirmed by viewing the injection schedule displayed on the monitor. The test engines are operated at a typical constant speed with various loads using different biodiesel fuel samples, as given in Table 3.

The air and fuel flow rates, the exhaust gas temperatures, the cylinder and fuel line pressure histories and the exhaust emissions are recorded under steady-state test conditions. The lubricant oil and cooling-water temperatures at the various loads are maintained at similar values for diesel and for Karanja biodiesel. The cooling-water temperatures varied from 60 °C to 100 °C with increasing load and their fluctuations remained within ± 3 °C. All the observations are taken carefully; their experimental uncertainties are evaluated using the standard procedure given by Holman[22] and are provided in Appendix 2. The experimental uncertainties evaluated for the parameters of interest are summarized in Table 7.

Test fuel specifications

The biodiesel fuel used in the present work is produced from a non-edible vegetable oil source, namely Karanja oil. Karanja (*Pongamia pinnata*) can be cultivated on any type of soil and has a low moisture demand and a high oil content (25–30%).[14] The Karanja biodiesel used in this study was procured locally from manufacturers in the Tamilnadu state of India, stored in air-tight containers and used for the engine experiments within 2–3 months of their procurement. The fatty acid methyl ester profile of the neat Karanja biodiesel was measured and analysed using a NuChrom gas chromatograph with a flame ionization detector. The biodiesel samples are prepared in accordance with the standard EN 14214:2008.[3] The measured composition results of Karanja methyl ester (KME) in comparison with other non-edible biodiesels, namely Jatropha methyl ester (JME) and poon methyl ester (PME), are provided in Table 4. It may be noted that the major constituents in KME are methyl oleate and linoleate. Among these fuels, KME has a higher percentage of longer-carbon-chain-length esters than those of JME and PME. However, KME has a lower polyunsaturated content than those of JME and PME.

The fuel properties of interest in combustion and performance estimation for Karanja biodiesel are given in Table 5. The densities and the viscosities of the fuels

Downloaded from pid.sagepub.com at University of Sydney on May 1, 2015

Table 4. Biodiesel fatty acid composition.

	Value for the following fatty acid methyl ester compositions									
	C16:0	C16:1	C18:0	C18:1	C18:2	C20:0	C20:1	C22:0	C24:0	Others
KME	9.74	—	6.36	52.57	16.98	2.87	1.81	1.57	8.07	—
JME[a]	14.20	1.40	6.90	43.10	34.40	—	—	—	—	—
PME[b]	12.01	—	12.95	34.09	38.26	—	—	—	—	2.7

KME; Karanja methyl ester; JME: Jatropha methyl ester; PME: poon methyl ester.
[a]From the work by Sarin et al.[23]
[b]From the work by Sanjid et al.[24]

Table 5. Properties of diesel, the biodiesels and the diesel–KME blend.

Property (units)	Value for the following fuels				
	Diesel	KME	K50D50	JME	PME
Chemical formula[a]	$C_{12}H_{26}$	$C_{18.26}H_{34.76}O_{1.99}$	$C_{15.13}H_{30.38}O_{0.99}$	$C_{18.68}H_{35.11}O_2$	$C_{18.82}H_{35.40}O_2$
Fuel-bound oxygen[a] (mass %)	—	11.16	6.93	10.95	10.88
Hydrogen-to-carbon molar ratio	2.16	1.90	2.00	1.87	1.88
Molecular mass[a]	170	286.32	228.16	291.81	293.76
Density (kg/m^3 at 40 °C)	830	890	850	865[b]	869[c]
Viscosity (cSt at 40 °C)	2.43	5.71	4.12	4.72[b]	3.9–4.0[c]
Cetane number[a]	50	57.17	53.58	53.83	57[c]
Lower calorific value (MJ/kg)	42.49	35.91[a]	39.2	39.82[b]	41.39[c]
Unsaturated-to-saturated ratio[a]	—	2.60	—	3.73	2.79
Iodine value[a,d]	—	75.88	—	97.97	97.12
Stoichiometric air-to-fuel ratio	14.93	12.44	13.37	12.44	12.46

KME; Karanja methyl ester; K50D50: 50 vol % Karanja biodiesel–50 vol % diesel; JME: Jatropha methyl ester; PME: poon methyl ester.
[a]Calculated from the compositional values.
[b]From the work bye Palash et al.[25]
[c]From the work by Sanjid et al.[24]
[d]From the standard EN 14214:2008.[3]

are measured using a hydrometer and a viscometer respectively according to the ASTM standards. The cetane numbers of the biodiesels are estimated in terms of their measured compositions using the Bamgboye et al.[26] correlation. The iodine values and calorific values of Karanja biodiesel are estimated on the basis of the standard EN14214:2008[3] and the Kays mixing rule respectively, based on the lower heating values of the methyl ester constituents taken from the literature.

Results and discussion

The measured data concerning the cylinder pressure histories, the fuel injection line pressures, the engine performances and the exhaust NO emissions with Karanja biodiesel (K100), 50% Karanja biodiesel–50% diesel (K50D50) blend and diesel are analysed and discussed below.

Figure 2(a) shows a typical comparison of the fuel line pressures using diesel and using Karanja biodiesel in full-load operating conditions.

The fuel line pressures are higher for Karanja biodiesel, probably owing to its higher density, which means that a higher mass of fuel is delivered from the mechanical-type fuel pump because the fuel is metered on a volume basis. Also, the timing of the start of dynamic fuel injection (the instant at which the line pressure attains 230 bar) is advanced for Karanja biodiesel, which could be due to its higher density and higher (approximately 17%) bulk modulus than those of diesel. As opined by earlier researchers,[11–15] a higher bulk modulus of biodiesel increases the velocity of sound wave propagation in the injection system and thus advances the injection timing. It is noted that the magnitude of the injection advance varied with the load up to a maximum of 2.6° CA in the 40% load condition (see Figure 2(b)). The measured cylinder pressure histories of diesel and of Karanja biodiesel are compared in Figure 3(a). The comparison shows an earlier start of combustion with a higher peak pressure rise for Karanja biodiesel. The deduced peak pressures in various test load conditions with diesel and with Karanja biodiesel show similar trends of higher peak pressures, as shown in Figure 3(b).

The higher peak pressure with Karanja biodiesel is primarily due to the early start of combustion owing to an advanced start of injection and a shorter ignition delay. When the combustion starts early, the occurrence of peak pressures are much closer to the top dead centre position during the expansion stroke and thus

Downloaded from pid.sagepub.com at University of Sydney on May 1, 2015

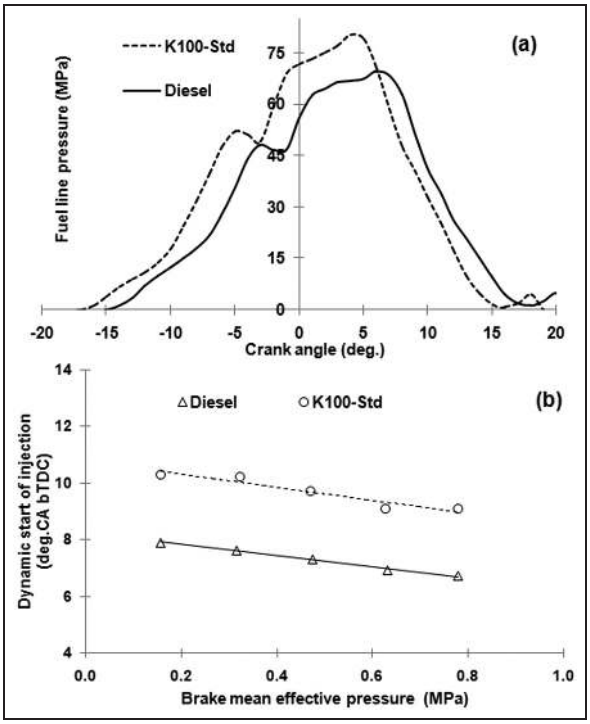

Figure 2. Comparison of (a) the fuel line pressures and (b) the start-of-injection timings with diesel and with Karanja biodiesel.
K100-Std: Karanja oil (biodiesel) with unaltered injection timing; CA: crank angle; bTDC: before top dead centre.

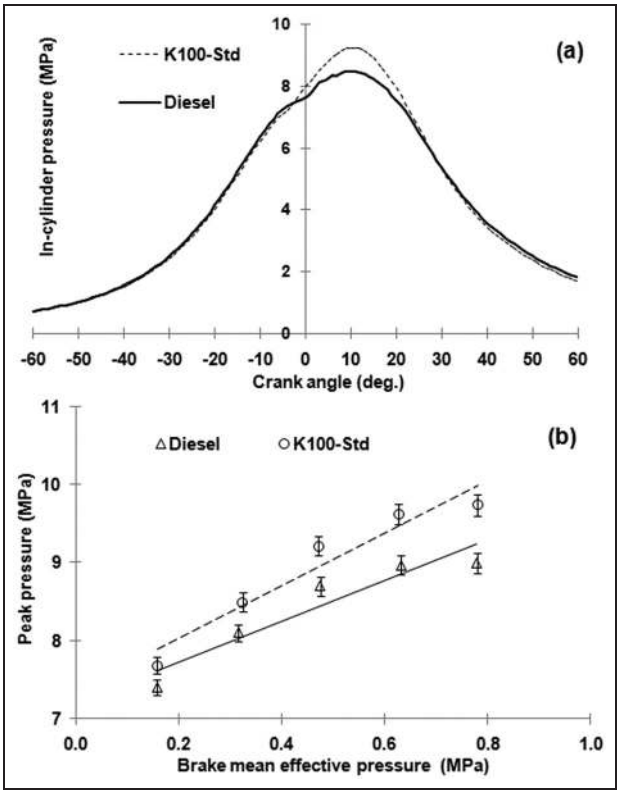

Figure 3. Comparison of (a) the cylinder pressures and (b) the peak pressures with diesel and with Karanja biodiesel.
K100-Std: Karanja oil (biodiesel) with unaltered injection timing.

are higher. In general, biodiesel fuels have higher cetane numbers than that of diesel and thus exhibit shorter ignition delays, as shown in Figure 4.

The average in-cylinder gas temperature histories for Karanja biodiesel and diesel fuels during the closed loop of the engine cycle are estimated by applying the ideal gas equation of state during the compression stroke and the first law of thermodynamics during combustion, and the results obtained are compared in Figure 5. As observed in the figure, the average in-cylinder gas temperatures are higher and its occurrence is advanced with Karanja biodiesel relative to diesel by around 5° CA. The average in-cylinder temperature trends are consistent with that of the cylinder pressure trends discussed earlier.

Figure 6 compares the measured brake specific nitric oxide (BSNO) concentrations of diesel and of Karanja biodiesel in the test load conditions. The NO emissions are higher for biodiesel at all loads with a maximum increase of 7.5% compared with those for diesel.

A higher NO for biodiesel correlates well with a higher peak cylinder temperature and its early occurrence, which provides a longer residence time for the high-temperature post-flame burned gases, favouring higher thermal NO formation. It should be highlighted here that the favorable in-cylinder conditions for a higher NO formation with biodiesel is primarily due to the advanced dynamic injection timing in the present mechanical-type injection system. Thus the changes in the in-cylinder charge conditions owing to an advanced

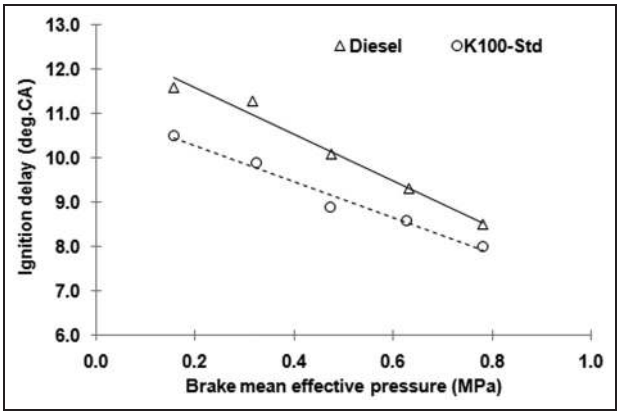

Figure 4. Comparison of the ignition delays with diesel and with Karanja biodiesel.
K100-Std: Karanja oil (biodiesel) with unaltered injection timing.

injection timing with biodiesel is a major contributor to its higher NO emissions. To extend the above claim, it was intended to retard the timing of injection manually during the biodiesel operation and to restore it to that of the diesel injection timing. The investigations pertaining to the changes in the in-cylinder charge conditions and the NO emissions with retarded injection timing using biodiesel will be discussed next.

The in-cylinder charge conditions at the time of fuel injection differ significantly at the standard timings and

Downloaded from pid.sagepub.com at University of Sydney on May 1, 2015

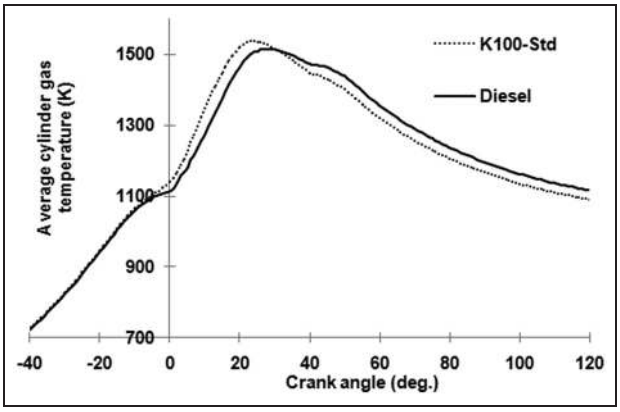

Figure 5. Comparison of the average cylinder gas temperatures with diesel and with Karanja biodiesel at full load.
K100-Std: Karanja oil (biodiesel) with unaltered injection timing.

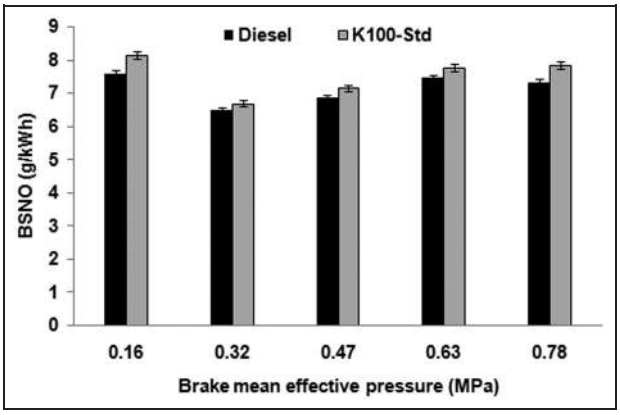

Figure 6. Comparison of the BSNO emissions with diesel and with Karanja biodiesel.
BSNO: brake specific nitric oxide; K100-Std: Karanja oil (biodiesel) with unaltered injection timing.

Table 6. In-cylinder charge conditions for KME at the start of injection.

Load (%)	Cylinder pressure (MPa)		Cylinder temperature (K)	
	Standard	Retarded	Standard	Retarded
20	4.65	5.12	678.22	729.12
40	5.16	5.72	696.98	736.49
60	5.74	6.37	719.06	741.57
80	6.18	6.61	733.81	749.05
100	6.40	6.84	739.66	751.10

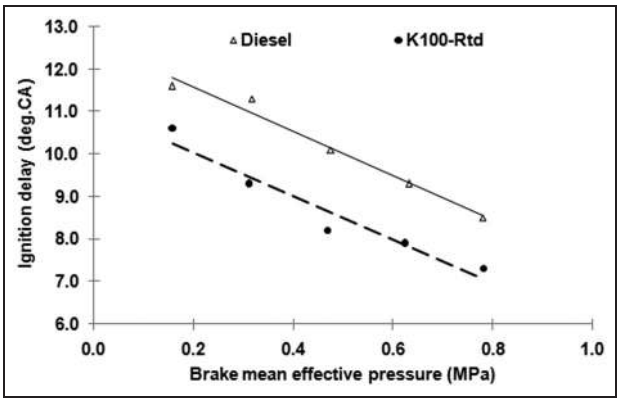

Figure 7. Comparison of the ignition delays with diesel and with Karanja biodiesel.
CA: crank angle; K100-Rtd: Karanja oil (biodiesel) with compensated injection timing.

the retarded timings, as given in Table 6. The charge pressures and temperatures at the start of injection are higher with retarded timings owing to the higher effective compression and hence the lower ignition delay (Figure 7).

Figure 8(a) shows a typical comparison of the measured cylinder pressure histories with diesel and with Karanja biodiesel in the full-load condition. It is observed that the cylinder pressures are of the same order of magnitude using the two fuels. Similar results are obtained in the other load conditions as reflected in the similar peak pressure values with diesel and with Karanja biodiesel, as shown in Figure 8(b). With the retarded injection timings using the Karanja biodiesel, the occurrence of the peak pressures are delayed during the expansion stroke and thus their magnitudes are smaller. From these trends, it is evident that, when the dynamic timings of the two fuels are maintained at similar values, the cylinder pressure levels have the same magnitudes.

The changes in the combustion parameters and the exhaust NO concentrations after the injection timing retard with Karanja biodiesel in comparison with the baseline results with diesel fuel under the standard injection timings are discussed next. The combustion phasing shown in Figure 9 is inferred from the cumulative energy release by considering the time elapsed for 50% energy release, which is useful for onboard combustion diagnosis and control. With the retarded injection timings, the combustion phasings with Karanja biodiesel are similar to those with diesel fuel up to 50% load and are early in higher-load conditions; this could be due to a higher burn rate with biodiesel on account of the fuel-bound oxygen.

The average in-cylinder gas temperature histories compared in Figure 10 for diesel and for Karanja biodiesel in the full-load condition show a lower gas

Downloaded from pid.sagepub.com at University of Sydney on May 1, 2015

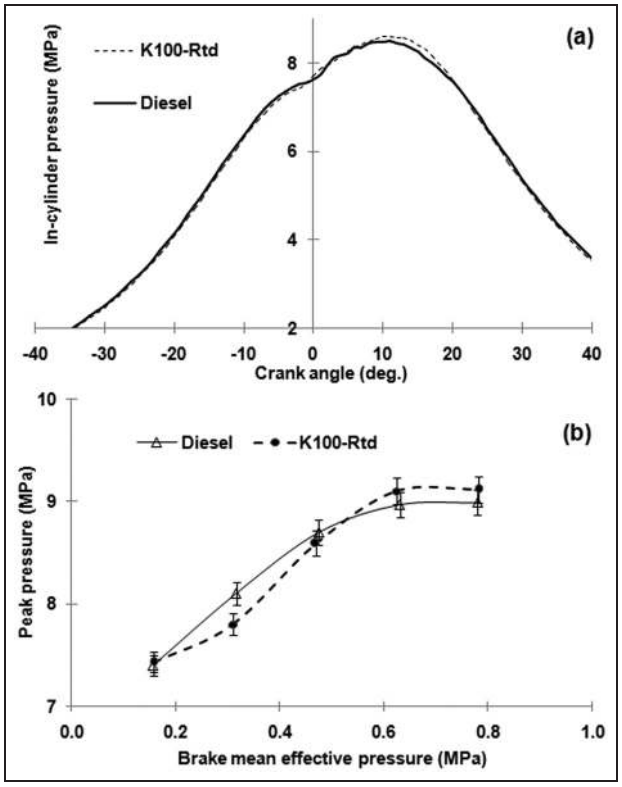

Figure 8. Comparison of (a) the cylinder pressures and (b) the peak pressures with diesel and with Karanja biodiesel.
K100-Rtd: Karanja oil (biodiesel) with compensated injection timing.

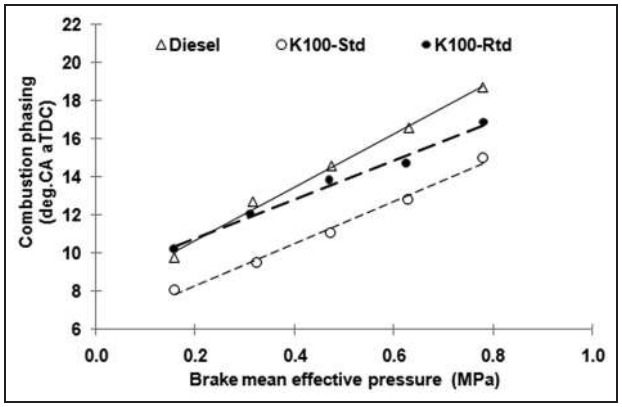

Figure 9. Comparison of the combustion phasings with diesel and with Karanja biodiesel.
CA: crank angle; aTDC: after top dead centre; K100-Std: Karanja oil (biodiesel) with unaltered injection timing; K100-Rtd: Karanja oil (biodiesel) with compensated injection timing.

temperature with Karanja biodiesel. Also, the timings of occurrence of the peak gas temperatures are similar for the two fuels. The fact that the average gas temperature of Karanja biodiesel is lower than that of diesel is primarily due to the shorter delay and the premixed combustion. Similar trends are obtained in the other load conditions, which are not presented here for brevity.

A comparison between the exhaust NO concentrations compared with diesel and with Karanja biodiesel

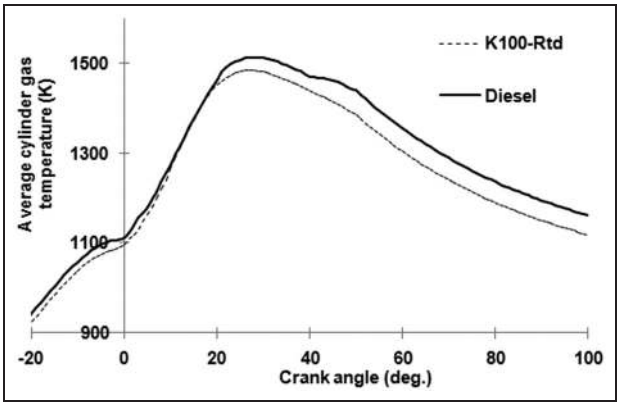

Figure 10. Comparison of the average cylinder gas temperatures with diesel and with Karanja biodiesel at full load.
K100-Rtd: Karanja oil (biodiesel) with compensated injection timing.

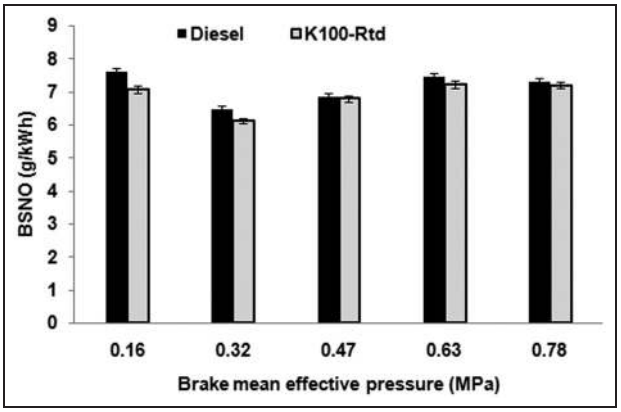

Figure 11. Comparison of the BSNO emissions with diesel and with Karanja biodiesel.
BSNO: brake specific nitric oxide; K100-Rtd: Karanja oil (biodiesel) with compensated injection timing.

in Figure 11 show similar vlaues or slightly lower values with biodiesel in the test load conditions. With the injection timing retard using Karanja biodiesel, the in-cylinder thermodynamic conditions in terms of the peak cylinder pressure, its occurrence and the peak gas temperature are restored to the same levels as with diesel fuel. As a result, the thermal NO formation processes are expected to be similar with diesel and with Karanja biodiesel. On the basis of these results, it can be concluded that the effect of other factors such as the differences in the spray characteristics and the fuel-bound oxygen contents of biodiesel have insignificant effects on its NO formation. It is evident that the bulk-modulus-dependent automatic advance in the dynamic injection timing with Karanja biodiesel under the standard injection time settings is a major contributor to its higher NO emissions.

To examine the fuel consumption penalty on account of the retarded injection timing, the brake specific fuel consumptions (BSFC) with standard and retarded timings with Karanja biodiesel in comparison with those of

Downloaded from pid.sagepub.com at University of Sydney on May 1, 2015

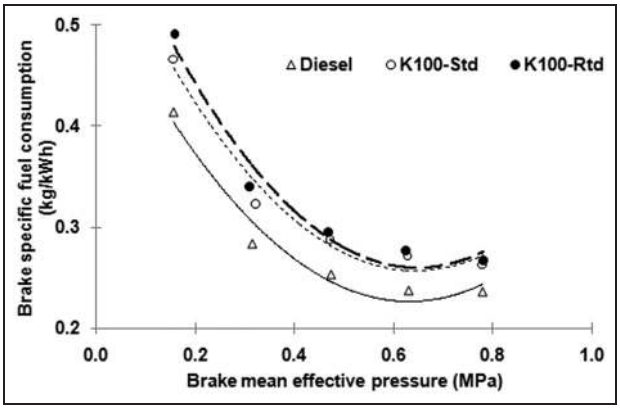

Figure 12. Comparison of the BSFCs with diesel and with Karanja biodiesel.
K100-Std: Karanja oil (biodiesel) with unaltered injection timing; K100-Rtd: Karanja oil (biodiesel) with compensated injection timing.

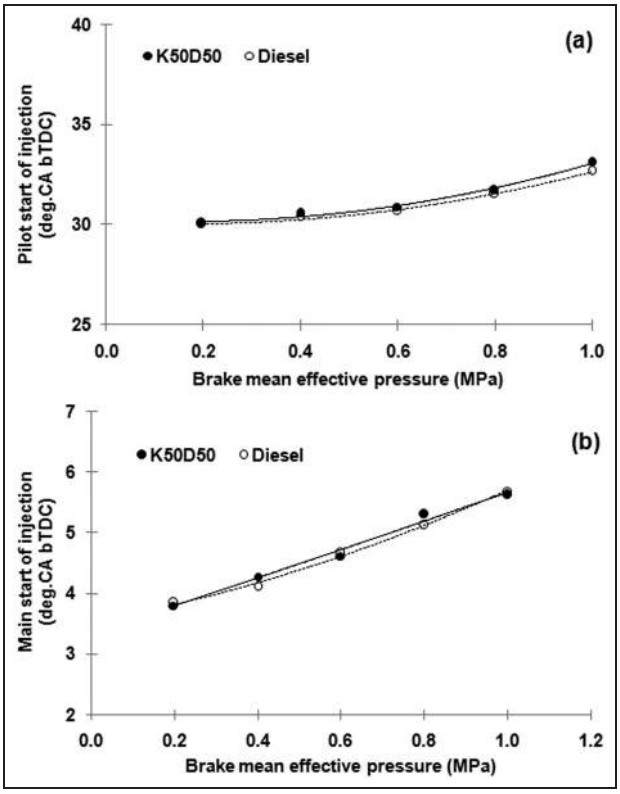

Figure 13. Comparison of (a) the pilot timimgs and (b) the main start-of-injection timings with diesel and with 50% Karanja biodiesel–50% diesel blend.
CA: crank angle; bTDC: before top dead centre; K50D50: 50% Karanja biodiesel–50% diesel.

diesel are presented in Figure 12. Although, the BSFC values are higher at low loads owing to the timing retard, they are of the same order of magnitude in higher-load conditions.

Having performed experiments on a mechanical-distributor-type injection system, an attempt was made to examine the biodiesel injection characteristics in a CRDI engine (engine B) using a 50% Karanja

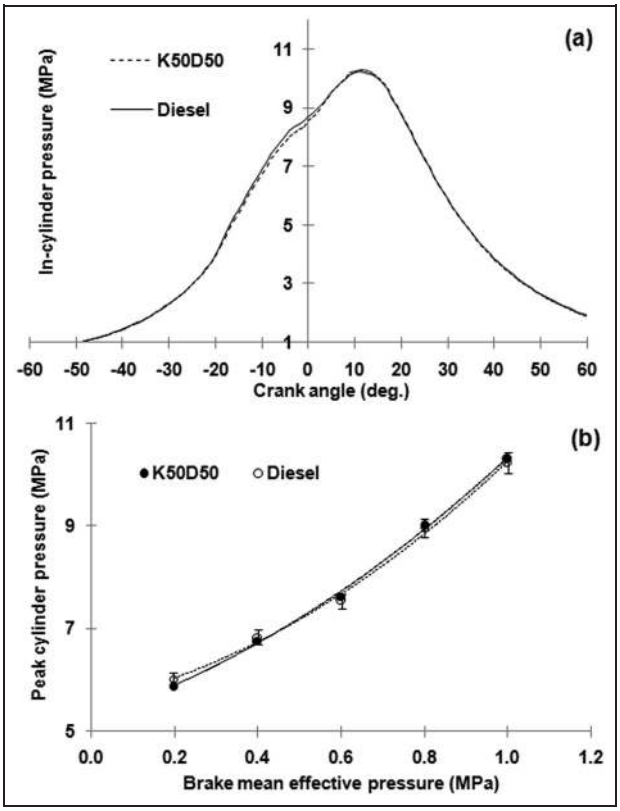

Figure 14. Comparison of (a) the cylinder pressures and (b) the peak pressures with diesel and with the 50% Karanja biodiesel–50% diesel blend.

biodiesel–50% diesel blend. It should be noted that a 50% biodiesel blend is used instead of neat biodiesel to avoid any operational difficulty due to the use of a high-viscosity fuel in a smaller-orifice injector. The use of a 50% Karanja biodiesel–50% diesel blend is justified in the light of the observations made concerning the biodiesel blends where a biodiesel–diesel blend with only up to 20% biodiesel is reported to behave like diesel, but beyond that the biodiesel property dominates. The combustion and NO emission characteristics of engine B using the 50% Karanja biodiesel–50% diesel blend are compared in order to examine the claim that the injection advance with Karanja biodiesel is the sole contributor to its higher NO emissions compared with the situation with diesel. The precisely controlled injection timings in the CRDI engine using an electronically operated injection system avoid injection timing differences between the two fuels due to the changes in their properties. The pilot and main injection timings for diesel and the 50% Karanja biodiesel–50% diesel blend are compared in Figure 13. As expected, the results show insignificant changes in both the pilot injection timings (see Figure 13(a)) and the main injection timings (see Figure 13(b)) for the two fuels in all the test load conditions.

The cylinder pressure histories in the full-load condition are identical for the two fuels, as shown in Figure 14(a). The deduced peak pressures in all the load

Downloaded from pid.sagepub.com at University of Sydney on May 1, 2015

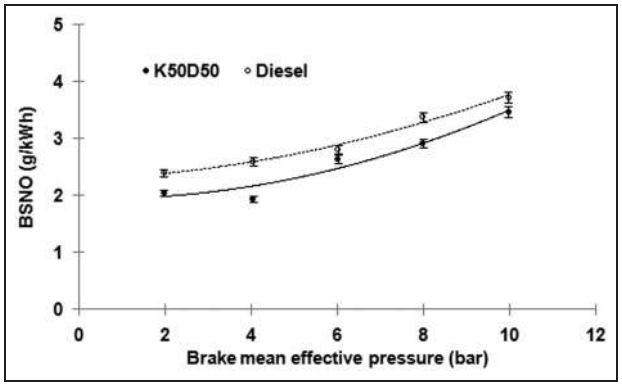

Figure 15. Comparison of the BSNO emissions with diesel and with the 50% Karanja biodiesel–50% diesel blend.
BSNO: brake specific nitric oxide; K50D50: 50% Karanja biodiesel–50% diesel.

conditions show similar values for the two fuels, as given in Figure 14(b).

Figure 15 shows the variation in the BSNO for diesel and for the 50% Karanja biodiesel–50% diesel blend in all the test load conditions. It is observed that the NO concentrations with the 50% Karanja biodiesel–50% diesel blend are either similar to or slightly lower than with diesel.

The biodiesel NO penalty as observed in a mechanical-type injection system is not encountered in a modern electronic injection system primarily because of the similar injection timings with diesel and with biodiesel and thus provides supportive evidence that the sole contributor to the biodiesel NO penalty is the favorable thermodynamic conditions for thermal NO formation owing to advanced injection timing.

Conclusions

The experimental investigations carried out to explore the major contributor to the biodiesel NO penalty using two different engines, one incorporating a mechanical-type injection system and the other incorporating an electronic-type injection system reveals the following.

1. Because of the higher bulk modulus of biodiesel, an advance in the dynamic injection timing up to a maximum of 2.6° CA is observed in the engine having a mechanical-type injection system which has contributed to higher specific NO emissions of 7.5%.
2. By restoring the injection timing of Karanja biodiesel to the same level as that of diesel, the NO concentrations are of the same magnitudes with the two fuels because of the similar thermodynamic conditions favouring thermal NO formation. This shows that the effects of other factors such as the differences in the spray characteristics and the fuel-bound oxygen content of biodiesel have insignificant effect on the NO formation.
3. NO neutrality of biodiesel is possible in engines with a mechanical-type injection system via tuning the injection timings without an expensive exhaust after-treatment system.
4. In a modern engine with an electronic-type injection system, the NO emission levels are similar with diesel and with the the 50% Karanja biodiesel–50% diesel blend.

Acknowledgements

The test engines provided by Eicher Motors and Ford Motors and the combustion instrumentation for the test set-up provided by Kistler are gratefully acknowledged.

Declaration of conflicting interests

The authors declare that there is no conflict of interest.

Funding

This research received no specific grant from any funding agency in the public, commercial or not-for-profit sectors.

References

1. Demirbas A. *Biodiesel: a realistic fuel alternative for diesel engines*. London: Springer, 2008, pp.111–117.
2. ASTM D6751 *Standard specification for biodiesel fuel blend stock (B100) for middle distillate fuels*. West Conshohocken, Pennsylvania: ASTM International, 2012.
3. EN 14214:2008 *Automotive fuels – fatty acid methyl esters (FAME) for diesel engines – requirements and test methods*. Brussels: Comité Européen de Normalisation, 2008.
4. Canakci M. Combustion characteristics of a turbocharged DI compression ignition engine fueled with petroleum diesel fuels and biodiesel. *Bioresource Technol* 2007; 98: 1167–1175.
5. US Environmental Protection Agency. A comprehensive analysis of biodiesel impacts on exhaust emissions. Report EPA420-P-02-001, Assessment and Standards Division, Office of Transportation and Air Quality US Environmental Protection Agency, Washington, DC, USA, October 2002.
6. Canakci M. NO_x emissions of biodiesel as an alternative diesel fuel. *Int J Veh Des* 2009; 50: 213–228.
7. Xue J, Grift TE and Hansen AC. Effect of biodiesel on engine performances and emissions. *Renewable Sustainable Energy Rev* 2011; 15: 1098–1116.
8. Boehman A, Alam M, Song J, et al. Fuel formulation effects on diesel fuel injection, combustion, emissions and emission control. In: *9th diesel engine emissions reduction conference*, Newport, Rhode Island, USA, 24–28 August 2003, pp. 1–9. Washington, DC: US Department of Energy.
9. Bittle JA, Knight BM and Jacobs TJ. Interesting behavior of biodiesel ignition delay and combustion duration. *Energy Fuels* 2010; 24: 4166–4177.
10. Knight BM, Bittle JA and Jacobs TJ. The role of system responses on biodiesel (palm olein) nitric oxide emissions in a medium-duty diesel engine. *Int J Engine Res* 2011; 12: 336–352.
11. Monyem A, Van Gerpen JH and Canakci M. The effect of timing and oxidation on emissions from biodiesel-fueled engines. *Trans ASAE* 2001; 44: 35–42.

Downloaded from pid.sagepub.com at University of Sydney on May 1, 2015

12. Canakci M and Van Gerpen JH. Comparison of engine performance and emissions for petroleum diesel fuel, yellow grease biodiesel and soybean oil biodiesel. *Trans ASAE* 2003; 46: 937–944.
13. Szybist JP, Boehman AL, Taylor JD, et al. Evaluation of formulation strategies to eliminate the biodiesel NO_x effect. *Fuel Processing Technol* 2005; 86: 1109–1126.
14. Anand K, Sharma RP and Mehta PS. Experimental investigations on combustion, performance, and emissions characteristics of a neat biodiesel-fuelled, turbocharged, direct injection diesel engine. *Proc IMechE Part D: J Automobile Engineering* 2009; 224(5): 661–679.
15. Dhar A and Agarwal AK. Performance, emissions and combustion characteristics of Karanja biodiesel in a transportation engine. *Fuel* 2014; 119: 70–80.
16. Sun J, Caton JA and Timothy J. Oxides of nitrogen emissions from biodiesel-fuelled diesel engines. *Prog Energy Combust Sci* 2010; 36: 677–695.
17. Ren Y, Abu-Ramadan E and Li X. Numerical simulation of biodiesel fuel combustion and emission characteristics in a direct injection diesel engine. *Front Energy Power Engng China* 2010; 4: 252–261.
18. Canakci M. Performance and emissions characteristics of biodiesel from soybean oil. *Proc IMechE Part D: J Automobile Engineering* 2005; 219(7): 915–922.
19. Hoekman SK and Robbins C. Review of the effects of biodiesel on NO_x emissions. *Fuel Processing Technol* 2012; 96: 237–249.
20. Palash SM, Kalam MA, Masjuki HH, et al. Impacts of biodiesel combustion on NO_x emissions and their reduction approaches. *Renewable Sustainable Energy Rev* 2013; 23: 473–490.
21. Palash SM, Masjuki HH, Kalam MA, et al. State of the art of NO_x mitigation technologies and their effect on the performance and emission characteristics of biodiesel-fueled compression ignition engines. *Energy Conversion Managmt* 2013; 76: 400–420.
22. Holman JP. *Experimental methods for engineers*. 7th edition.New York: McGraw-Hill, 2007, pp. 51–65.
23. Sarin R, Sharma M, Sinharay S and Malhotra RK. Jatropha–palm biodiesel blends: an optimum mix for Asia. *Fuel* 2007; 86: 1365–1371.
24. Sanjid A, Masjuki HH, Kalam MA, et al. Impact of palm, mustard, waste cooking oil and *Calophyllum inophyllum* biofuels on performance and emission of CI engine. *Renewable Sustainable Energy Rev* 2013; 27: 664–682.
25. Palash SM, Kalam MA, Masjuki HH, et al. Impacts of NO_x reducing antioxidant additive on performance and emissions of a multi-cylinder diesel engine fueled with Jatropha biodiesel blends. *Energy Conversion Managmt* 2014; 77: 577–585.
26. Bamgboye AI and Hansen AC. Prediction of cetane number of biodiesel fuel from the fatty acid methyl ester (FAME) composition. *Int J Agrophys* 2008; 22: 21–29.

Appendix 1

Q_{net}	net heat release rate

Abbreviations

aTDC	after top dead centre
bTDC	before top dead centre
BMEP	brake mean effective pressure
BSFC	brake specific fuel consumption
BSNO	brake specific nitric oxide
CA	crank angle
CRDI	common-rail direct injection
JME	Jatropha methyl ester
K50D50	50 vol % Karanja biodiesel–50 vol % diesel
KME	Karanja methyl ester
K100-Std	Karanja oil (biodiesel) with unaltered injection timing
K100-Rtd	Karanja oil (biodiesel) with compensated injection timing
NO	nitric oxide
NO_x	nitrogen oxides
PME	poon methyl ester
SOI	start of injection

Appendix 2

The experimental uncertainty values estimated for the measured quantities involved in this study are provided in Table 7.

Table 7. Measurement uncertainty.

Parameter	Uncertainty (%)	
	Engine A	Engine B
Speed (r/min)	± 0.24	± 0.07
Brake torque (N m)	± 2.02	± 1.02
Fuel time (s)	± 1.06	± 3.06
Air time (s)	± 1.06	± 0.26
Exhaust gas temperature (°C)	± 2.28	± 0.43
Lubricant oil temperature (°C)	± 1.55	± 0.95
Cooling water temperature (°C)	± 2.71	± 3.27
BSNO (g/kW h)	± 1.45	± 2.64

BSNO: brake specific nitric oxide.

Downloaded from pid.sagepub.com at University of Sydney on May 1, 2015